Rock mechanical aspects for cavern stability

T. Pilgerstorfer
Amberg Engineering AG. Regensdorf, Switzerland

H. Wannenmacher
Amberg Engineering AG. Sargans, Switzerland

K. Grossauer
Amberg Engineering AG. Regensdorf, Switzerland

A. Stucki
AF-Consult Switzerland AG, Baden, Switzerland

B. Schwegler
KWO Kraftwerke Oberhasli, Innertkirchen, Switzerland

ABSTRACT: The extension of Grimsel 3 hydropower project (600 MW) foresees the construction of a 2.5 km long tailrace tunnel, a machine and the transformer cavern as well as a new 600 m deep vertical shaft connecting the existing conduit with the Räterichsboden reservoir. General high in situ stress conditions are expected for the construction of the extension of the Grimsel 3 hydropower project within the massive Grimsel granodiorite and granite. Due to higher ground coverage for the cavern structure, in the course of the relocation for the vertical shaft, brittle rock mass behaviour is expected influencing the construction. The specific intact rock and rock mass conditions as well as the stress conditions were investigated with 600 m deep core drillings in order to obtain the geomechanical conditions and parameters at cavern structure level. The investigation included detailed analyses of brittle rock parameters as well as in situ hydro-fracturing tests. Brittle parameters of rock were utilized for the two and three dimensional finite element analyses to determine depth of spalling and fracturing expected for the construction. The variances of the two and three dimensional finite element analyses as well as the influence of brittle parameters influencing the analyses are discussed.

1 INTRODUCTION

The pump storage plant (PSP) Grimsel 3 will connect the existing pressure tunnels of the PSP Grimsel 2, built in the late 1970's with the reservoir of Räterichsboden. The installed capacity of the Grimsel 3 PSP is approximately 660 MW with an expected flow rate of 130 m^3/s. The major construction elements of the pump storage scheme to develop are the approximately 550 m deep vertical pressure shaft, the tailrace tunnel with a length of about 2.5 km and the power house complex.

2 PLANT LAYOUT

Due to the utilization of a vertical shaft the galleries of Grimsel III are situated deep within the ridge of the "Schwarze Nollen". The overburden at the cavern structure is approximately 650 m. The cavern layout foresees a separation of the machine and the transformer cavern, which is situated above the tailrace galleries. The caverns are connected via three small galleries. Three variable speed pumping turbine will be used for electricity production and pumping. The ratio of width to height and length for the machine cavern is 27.6 * 46.6 * 92.5 m and 18.1* 30.9 * 112.6 m for the transformer cavern. The machine cavern also hosts three upstream spherical valves, where else the three butterfly valves are situated in the transformer cavern. All access tunnels to the underground structure are connected to the existing structures of the KWO, guaranteeing access all time of the year within this high altitude construction area. The access tunnels are further utilized for ventilation, drainage, escape paths and for energy transmission.

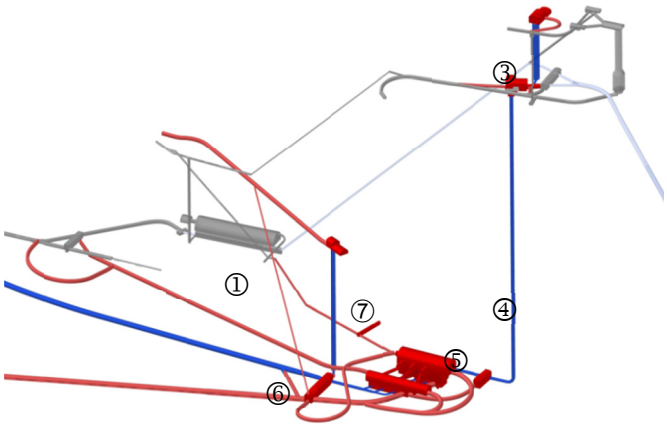

Figure 1. Grimsel 3 Structure.

The main elements of the structure are as follows:

① Cavern Structure Grimsel 2
② Pressure Tunnel up-stream
③ Surge Shaft Grimsel 2 and Grimsel 3
④ Vertical Shaft up stream
⑤ Cavern Structure Grimsel 3
⑥ Tailrace Tunnel
⑦ Surge shaft down stream

3 GEOLOGICAL CONDITIONS

The project area is completely situated within the Swiss Aar massive. The rock units comprise of Magmatides, which intruded into the crystalline rock mass. The intake structure in the lake of "Räterichsboden" to the north is located at the boundary of the central Aare granite and the intruded Grimsel Granodiorite in the south. In order to establish a reliable geological and geotechnical model a vertical borehole extending to the depth of the planned cavern structure of Grimsel 3 was drilled to investigate the conditions below the existing structure of Grimsel II. The rock structure, as encountered, is characterised by a subdominant parallel foliation texture due to alpine deformation. The foliation is dipping steep to SSE. The fracture intensity is very low and the overall rock-mass conditions are massive with large interlocking blocks with a generally low permeability in the range of $10E^{-9}$ m/s up to $10E^{-14}$ m/s. Due to the dense characteristic of the rock mass, no crack water table is expected in the area, with overall dry and damp conditions for the tunnelling works.
The orientation of the geological structures towards the cavern orientation is subordinate influence on gravitational driven stability problems.

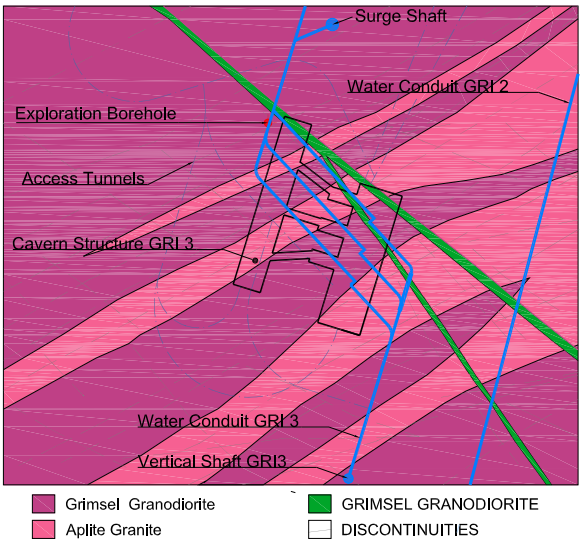

Figure 2. Geological conditions.

3.1 *Rock types*

The main rock types within the area are granodiorite, a coarse grained gneiss and minor aplitic medium grained, slightly foliated gneiss. The brittle behaviour of these rock types were investigated by intense rock mechanical testing performed at the ETH Zürich and EPF Lausanne. The rock types show a general small distribution in strength. The typical values for intact rock are summarized for granodiorite and aplitic gneiss in Table 1.

Crack initiation for the rock types is found approximately at 50 % of the intact rock strength.

Table 1. Typical values for rock types.

	Unit	Grano-diorite	Aplitic Gneiss
UCS, dry	[MPa]	130 - 150	180 - 190
UCS, wet	[MPa]	~110	~180
BT	[MPa]	7.0 - 12.5	9.0- 12.0
Unit weight	[g/cm^3]	2.73	2.61
Porosity, 48 h	[%]	0.26	0.31
Porosity, 4 mo.	[%]	0.34	0.51
E50, tangent, dry	[GPa]	56	56
E50, tangent, wet	[GPa]	49	53

4 GEOMECHANICAL MODEL

The construction of Grimsel 2 as well as the outputs of NAGRA test facility gives a detailed insight of the geomechanical boundary conditions for the design on the Grimsel 3 hydropower extension. The Grimsel area is well known for the high tectonic stresses, which is indicated by various surface parallel detachments and sudden bursts during construction of open excavations. Egger (1980) reports on stress induced failure (surface parallel spalling) occurred during the construction of Grimsel II cavern at the transition of the sidewalls to the invert. Numerical back (internal document) calculations could reproduce the spalling mainly located at the stress raisers of the shallow placed cavern structure. All underground structures of the KWO are situated more or less near surface, allowing no prediction of stress development for Grimsel III cavern structure. Minor water ingress occurred during the heading of the access tunnel of Grimsel 2.

4.1 *Initial Stress Conditions*

Especially in steep alpine morphologies, the primary stress state is influenced by the shape of the valley (absence of lateral confines of the slope), the tectonic history and the elastic properties of the gneisses. The initial stress conditions (magnitude and orientation) may significantly affect the cavern stability in case of unfavourable orientation. In total, seven hydraulic fracturing tests were conducted at the 600 m deep borehole providing essential information of the local stress. The orientation of the stress field varies within the area where else the magnitude of the stress data is in line with the overall stress regime (see Fig. 3). The general orientation of the major horizontal stress is about E - W with a magnitude of two (in fractured zones) to three times (in massive zones) exceeding the vertical stress within the depth of the cavern. Local borehole breakouts at the depth of the cavern prove the orientation of the hydraulic fracturing analyses.

The minimum primary stress is oriented more or less parallel to the vertical axis of the shaft with a magnitude of ~17.5 MPa at the low point, corresponding to an overburden of 650 m (Fig. 3).

The hydraulic fracturing analyses indicates following for the stress state (Evans 2012, Tab. 2).

Table 2. Magnitude and orientation of the stress state.

Grimsel 3	Primary Stress Regime
Magnitude	σ_h = z*(0.035618 ± 0.00544) σ_H = z*(0.05653 ± 0.0116) (pore-pressure considered) σ_H = z*(0.066624± 0.0116) (no pore-pressure considered)
Orientation	Azimuth σ_h [°] = 171 (average values) Azimuth σ_H [°] = 81 (average values)

The stress measurements fit in well with the general trends of the Grimsel area, with documented measurements from NAGRA test site (Bräuer et al. 1989) and various investigation campaigns and construction phases of hydropower plants in the area in the past few decades.

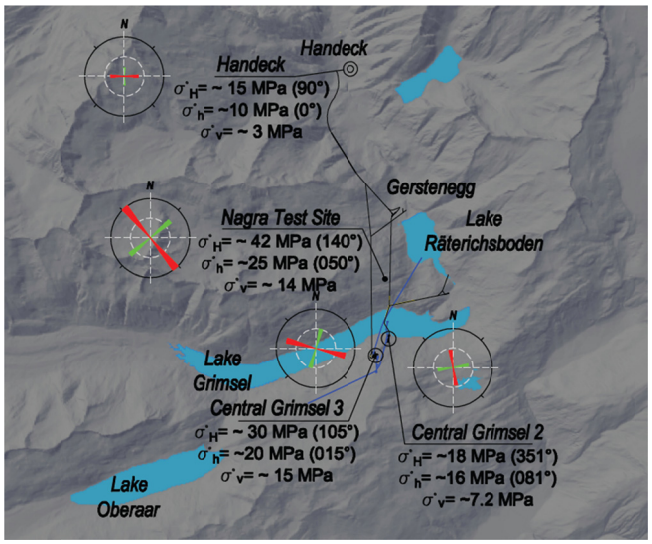

Figure 3. Stress regime in Grimsel area.

5 GEOTECHNICAL DESIGN

The geotechnical design was carried out according to Swiss Code SIA 199 (1998) in combination with the Austrian guideline for geotechnical design of underground structures (Austrian Society for Geomechanics 2008).

The geotechnical design considers the unsupported underground facility, the stress state and the orientation of the structures as well as groundwater conditions for stability analyses for the identification of hazard scenarios.

System behaviour is considered as the underground structure with all temporary or permanent rock support elements.

5.1 *Rock mass behaviour*

The expected rock mass behaviour for the construction of the caverns and adjacent structures is mainly associated to brittle failure (spalling and rock burst) and minor structural controlled overbreaks due to gravitational sliding and falling of blocks.

5.1.1 *Brittle failure (spalling, rock burst)*

Brittle failure as spalling and rock burst is generally associated with massive rock mass conditions and high stress regimes. Brittle failure is triggered by the exceedance of the tensile strength (Martin 1997, Diederichs 2002), with a failure pattern parallel oriented to the tunnel surface. Brittle failure is governed by the ratio of intact tensile (σ_t) and compressive (σ_{ci}) rock strength, crack initiation of intact rock strength as well as blockiness of rock mass GSI > 75 (Diederichs & Carvalho 2007) , expressed as block volume in relation to the underground opening.

As a criteria for brittle failure analyses Diederichs & Carvalho (2007) suggest a relationship of the ratio of σ_{ci} and σ_t and the GSI value (Tab. 3).

Table 3. brittle failure analysis criteria after Diederichs & Carvalho (2007).

σ_{ci}/σ_t	GSI			
	< 55	55 - 65	65 - 80	> 80
< 8	GSI	GSI	GSI	GSI
9 – 15	GSI	GSI	GSI	GSI/SP
15 – 20	GSI	GSI/SP	SP/GSI	**SP**
> 20	GSI	GSI/SP	SP	SP

GSI … rock mass strength according to GSI-value
SP … brittle failure analysis

The ratio of the tensile to the compressive strength in regard to the very massive ground conditions highlights the potential for stress induced failure.

5.1.2 *Constitutive law for estimation of spalling in highly stressed rock mass*

For the assessment of brittle failure the strength parameters at lower boundary of the distribution as well as values with the highest confidence are considered.

The brittle failure analysis reconciliates the history of the stress points, determined by a numerical 3D analysis, with the tri-linear constitutive law, proposed by Diederichs (2002). The formulation of the individual failure criteria for damage initiation, spalling limit, tensile and shear failure is given in Table 5.

Table 4. Rock mass parameters Grimsel Granodiorite.

Rock mass parameters		Unit	Value
rock mass strength	σ_{cm}	[MPa]	44
tensile strength rock mass	σ_{tm}	[MPa]	-0.9
Young`s Modulus rock mass	E_m	[GPa]	30
friction angle	φ	[°]	48
cohesion	c	[MPa]	14
Unit weight	ρ	[kN/m³]	27
Poisson's ratio	ν	[-]	0.19
Rock mass permeability	k	[m/s]	1xE-9
Dilatancy angle	ψ	[°]	0

Table 5. Formulation of the brittle failure criteria.

Damage threshold	$\sigma_1 = (d_i)\sigma_c + (1.0)\sigma_3$ *damage initiation* $d_i = 0.5$
Spalling limit	$\sigma_1 = (10)\sigma_3$
Shear failure (HB)	$\sigma_1 = \sigma_3 + \sigma_{cm}(m_b{*}\sigma 3/\sigma_{cm}+s)^a$ *for GSI = 80,* σ_{ci} *= 130 MPa,* σ_{cm} *= XX MPa,* m_i *= 29, a = 0.501,* m_b *= 14.197 and s = 0.1084* [1]
Tensile failure	$\sigma_t = 10$ MPa

Following principle failure modes can be distinguished with the σ_1 and σ_3 quadrant (Tab. 6).

Table 6. Principle failure modes after Diederichs (2002).

No failure Ⓐ	stress points do not exceed the damage initiation threshold.
Damage initiation Ⓑ	stress points exceeds the spalling limit and is situated above the damage threshold and below shear failure line.
Shear failure Ⓒ	stress points is situated above the shear failure line.
Spalling failure Ⓓ	stress point is above damage threshold, left of spalling limit and below shear failure.
Tensile failure Ⓔ	stress points exceed the tensile strength of intact rock.

Figure 4 depicts three regions – upper strength limit at high compression (shear failure), lower strength limit at low compression (in situ-strength), and limit at the passage to spalling failure.

[1] *(calculation according to Hoek and Brown faiure criterion (Hoek et.al. 2002)*

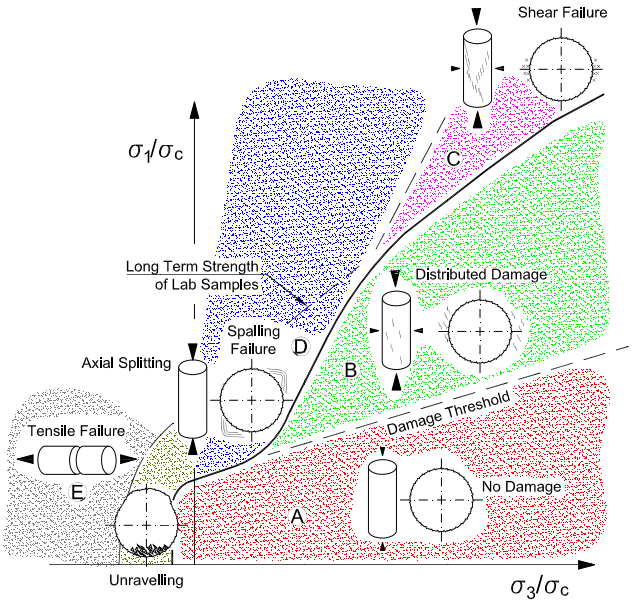

Figure 4. Compilation of strength envelopes for brittle rocks (modified from Diederichs 2002).

5.1.3 *Numerical Analyses*

A 3D numerical calculation was performed utilizing the finite difference program FLAC^{3D} (Itasca 2009) to investigate rock mass behaviour and define support requirements. The rock mass features a linearly elastic material behaviour. This simplification was deemed to be valid, since the rock mass strength is relatively high, with no expectation of plastification of the rock mass. The model considers beside cavern structure and the water conduit, some of the mayor access tunnel (Fig. 5).

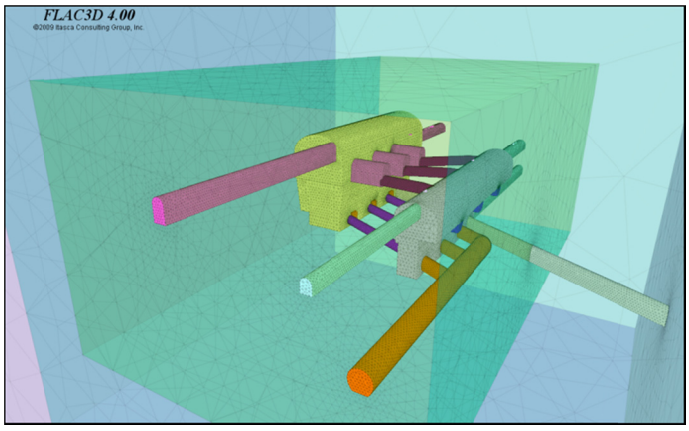

Figure 5. Overview 3D numerical model.

5.1.3.1 Results brittle failure analysis

The results of the brittle failure analysis are depicted as contour plots, where the different colours represent certain failure types (Fig. 6). The results show a plausible and for such rock mass conditions a typical and coherent behaviour.

Brittle failure (shallow overstressing of the rock mass) and spalling is present in the crown towards the haunches and, somewhat less pronounced in the

invert due to the high rock mass quality in combination with the dominating stress situation.

The highest tangential stresses are expected to occur in the crown/invert region (due to orientation of the major normal stress σ_h situated orthogonal to the cavern axis). In the corner zones of the cavern an exceedance of the tensile strength can be observed. The presence of such zones is often not visually apparent, however, its existence was proven through systematically observation of acoustic emissions and differences in wave propagation speed. The rock mass in such zones features lower cohesion, while the frictional properties generally remain the same (Martin 1997).

Since all failure modes mentioned above appear just in the vicinity of the excavations, the system behaviour can be deemed as stable without far reaching problems in a rock mechanical aspect or for the excavation.

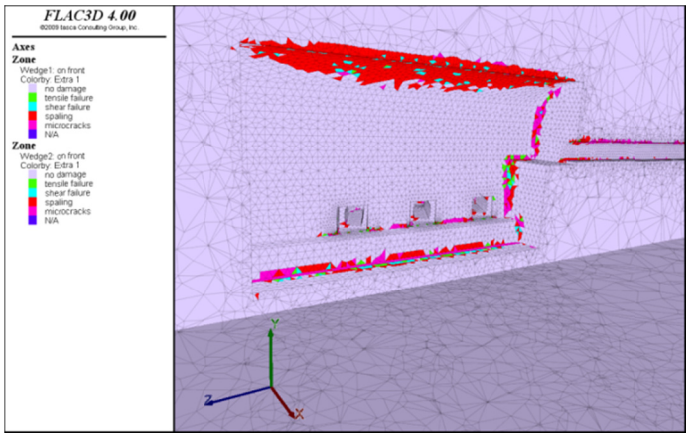

Figure 6. contour plot brittle failure analysis for the machine cavern (viewing direction headwater).

The results of the calculation with the parameters of Granodiorite with pre-existing joints show slightly less zones with occurrence of brittle failure. This is as expected since stress redistribution diminishes on the pre-existing discontinuities.

5.1.3.2 Support measures

The support concept of the cavern considers mainly potential wedge failure and effects of stress induced failure and resulting dead loads. A shotcrete lining consisting of four layers of shotcrete with wire- mesh each ten centimetres and staggered rock bolts with a length of 6 m and 12 m in the crown and 12 m at the side-walls. The grid of the bolts is 1.7*1.7 m in the crown and widened to 2.0*2.0 m at the sidewalls (Fig. 7).

The shotcrete was modelled as shell elements, which allow bearing of normal forces and bending moments, featuring linearly elastic material behaviour. The parameters for the shotcrete considered are given in Table 7.

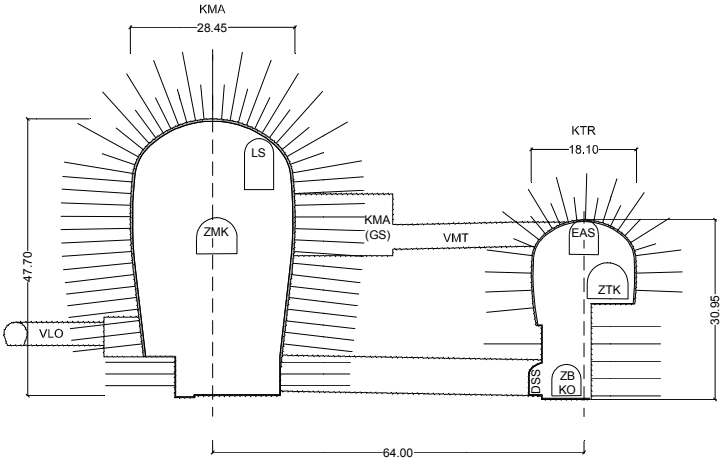

Figure 7. Simplified section of machine cavern (KMA) and transformer cavern (KTR).

Table 7. Shotcrete properties.

Shotcrete properties		Unit	Value
Young's Modulus	E_{SC}	[MPa]	7000
Compressive strength	$\sigma_{c,SC}$	[MPa]	30
Tensile strength	$\sigma_{t,SC}$	[MPa]	0.2
Poisson's ratio	ν		0.2
Unit weight	γ	[kN/m³]	25

The rock bolts are modelled as cable elements. The material behaviour is described by the behaviour of the steel and the grout independently. The bond stiffness and the bond strength between bolt, mortar and rock mass are considered in this formulation. The parameters for the mortar and the bolts are shown in Table 8 and Table 9, respectively.

Table 8. Anchor mortar parameters.

Anchor mortar parameters		Unit	Value
Diameter borehole	d_B	[mm]	51
Young's modulus	E_M	[MPa]	30000
Compressive strength (24 h)	σ_M	[MN]	25
Shear strength	τ_M	[MN]	0.32
Cohesion	c_M	[MPa/m]	2.00
Shear stiffness	G_M	[MPa]	11000
Unit Weight	γ	[kN/m³]	XX

Table 9. Bolt properties.

Bolts properties		Unit	Value
Diameter	d_A	[mm]	25
Young's modulus	E_A	[MPa]	210000
Max. tensile load	$F_{A,m}$	[MN]	0.4
Tensile load at yield stress	$F_{A,eh}$	MN	0.32
Unit weight	γ	[kN/m³]	78.50

The excavation steps of the caverns and adjacent access tunnels was modelled by a sequential removal of predefined clusters. The support is installed step by step in order to derive a realistic system behaviour of the excavation works (Fig. 8).

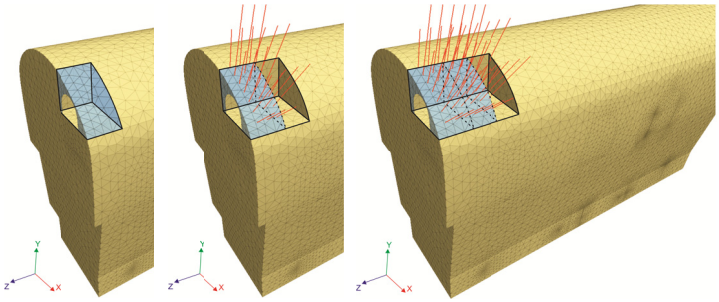

Figure 8. Sequential installation of initial widening of cavern.

Three main phases of the cavern excavation considering expected displacements as well as shotcrete and rock bolt utilization are analysed towards system behaviour. The investigated phases for the machine cavern are as follows:

- Phase A: Calotte excavation and support installation finished
- Phase B: Calotte and bench (level KMA) excavation and support installation finished (Fig. 9)
- Phase C: Excavation and support installation finished

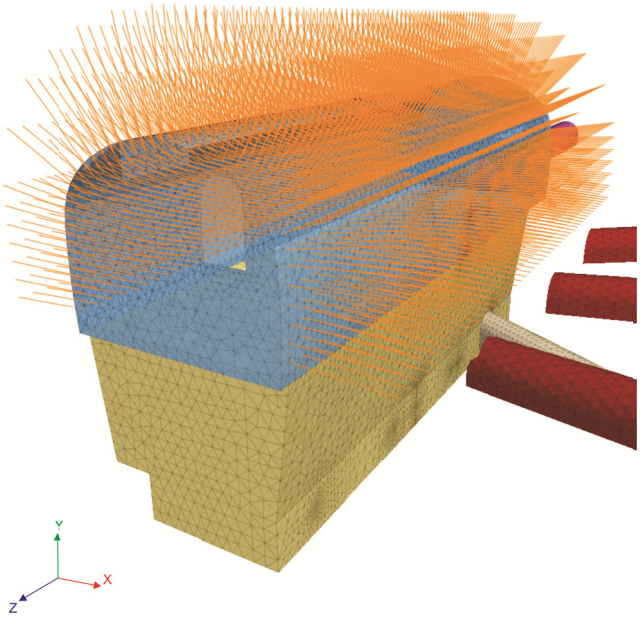

Figure 9. Excavation and support installation KMA Phase B.

The shotcrete experiences only a minor utilization during the calotte excavation (Phase A). Maximal normal forces to occur at the haunches are expected within the range of 2.0 MN. Maximum Anchor loads in the haunches are expected with a maximum of 65 kN, which is up to a utilisation of 20 % of the tensile load at yield strength. Normal forces will increase to about 3.0 MN in the haunches, where else no significant increase of normal force is found in the crown. The results are reasonable and in line with the orientation and magnitude of the initial stress state normal to the side wall. Due to displacements at the sidewalls in the range of 16 mm, some tensile stress is arising in the range of 2.5 MN. The crown area experiences no further stress rises at this stage. Maximum anchor loads at the haunches will increase to approximately 90 kN.

Displacements will further rise to a maximum value of about 30 mm at the sidewalls, expected at the half height of the cavern. Displacements at the crown will stabilize at a range of 2.5 to 3.0 mm (Fig. 10).

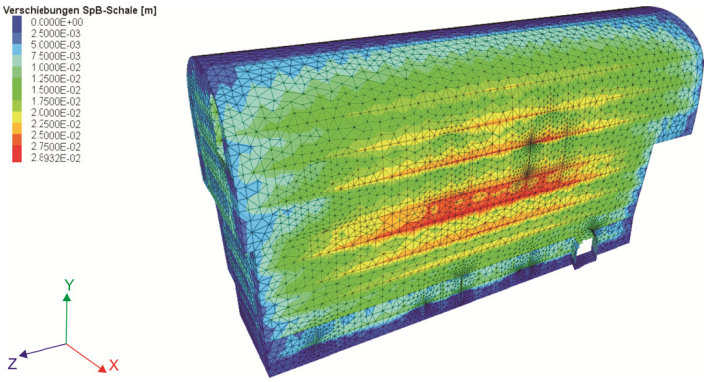

Figure 10. Displacements, Phase C.

Maximum normal loads of 3 MN are expected upon full excavation in the crown region. Tensile stress at the side wall will rise to magnitude of about 2 – 4 MN, without no mayor moments occurring in the lining. Maximum anchor loads will be expected within a range of 90 kN at the haunches towards the half height of the cavern. Anchors will be utilized at local areas up to a level of about 30 % of tensile load at yield strength.

6 CONCLUSION

The detailed analyses of ground behaviour utilizing 3D finite element modelling is a valuable method for the design of large underground structures. The output of the 3D dimensional compared with the standard 2D provides a more realistic view on expected behaviour. The implementation of brittle failure analyses within FLAC^{3D} proofed as a valuable analysis for rock mass behaviour and further on sufficient separation of underground structures to avoid undesired influences during excavation.

ACKNOWLEDGEMENTS

The assistance of Dr **F**. Amann on brittle failure discussion as well as Dr. HJ Ziegler in terms of the development of a geological and geotechnical model for the pump storage scheme is highly appreciated. All works for the design of the hydropower plant Grimsel III were performed by the EC GRI3 consisting of AF-Consult Switzerland AG, Gruner Ltd and Amberg Engineering Ltd.

7 REFERENCES

Austrian Society for Geomechanics. 2008. Guideline for the geotechnical design of underground structures with cyclic excavation. 2nd revised edition. Salzburg.

Bräuer, V., Kilger, B. & Pahl, A. 1989. Nagra Technical Report NTB 88-37E. Nagra, Baden.

Diederichs, M.S. & Carvalho, JL 2007. A modified approach for prediction of strength and post yield behaviour for high GSI rock masses in strong, brittle ground. *Proc. 1st Canada/U.S. Rock Mech. Symp. 2007*, Taylor & Francis Ltd, Vancouver, 249-257.

Diederichs, M.S. 2002. Keynote – stress induced accumulation and implications for hard rock engineering. In: Hammah R, Bawden WF, Curran J, Telsnicki M (eds.). Proc. NARMS 2002. Toronto: University of Toronto Press; 2002. pp. 3-14.

Egger, P. 1980. Schlussbericht über die durchgeführten felsmechanischen Untersuchungen (in german), Kraftwerke Oberhasli AG.

Evans, K. 2012. Evaluation of stress estimates, Kraftwerke Oberhasli AG.

Hoek, E., Carranza-Torres, C., & Corcum, B. 2002. Hoek-Brown criterion - 2002 edition. Proc. NARMS-TAC Conference, Toronto, 2002, 1, 267-273.

Itasca Consulting Group, Inc. 2009. FLAC3D Fast Lagrangian Analysis of Continua in 3 Dimensions, manual, 4th edition. Minnesota, USA.

Martin, C.D. 1997. The effect of cohesion loss and stress path on brittle rock strength, Canadian Geotechnical Journal Vol. 34, No. 5.